Gapless spin-liquid phase in the kagome spin-$\frac{1}{2}$ Heisenberg antiferromagnet

Yasir Iqbal,[1,2,*] Federico Becca,[3,†] Sandro Sorella,[3,‡] and Didier Poilblanc[2,§]

[1] *The Abdus Salam International Centre for Theoretical Physics, P. O. Box 586, I - 34151 Trieste, Italy*
[2] *Laboratoire de Physique Théorique UMR-5152, CNRS and Université de Toulouse, F-31062, Toulouse, France*
[3] *Democritos National Simulation Center, Istituto Officina dei Materiali del CNR and SISSA – International School for Advanced Studies, Via Bonomea 265, I-34136 Trieste, Italy*

(Dated: October 30, 2012)

We study the energy and the static spin structure factor of the ground state of the spin-1/2 quantum Heisenberg antiferromagnetic model on the kagome lattice. By the iterative application of few Lanczos steps on accurate projected fermionic wave functions and the Green's function Monte Carlo technique, we find that a gapless (algebraic) $U(1)$ Dirac spin liquid is competitive with previously proposed gapped (topological) $\mathbb{Z}_2$ spin liquids. By performing a finite-size extrapolation of the ground-state energy, we obtain an energy per site $E/J = -0.4365(2)$, which is equal, within three error-bars, to the estimates given by density-matrix renormalization group (DMRG). Our estimate is obtained for a translationally invariant system, and, therefore, does not suffer from boundary effects, like in DMRG. Moreover, on finite toric clusters at the pure variational level, our energies are lower compared to those from DMRG calculations.

PACS numbers: 75.10.Jm, 75.10.Kt, 75.40.Mg, 75.50.Ee

Introduction. The spin-1/2 quantum Heisenberg antiferromagnet (QHAF) on the kagome lattice provides a conducive environment to stabilize a quantum paramagnetic phase of matter down to zero temperature, [1–3] a fact that has been convincingly established theoretically from several studies, including exact diagonalization, [4–8] series expansion, [9, 10] quantum Monte Carlo, [11] and analytical techniques. [12] The question of the precise nature of the spin-liquid state of the kagome spin-1/2 QHAF has been intensely debated on the theoretical front, albeit without any definitive conclusions. Different approximate numerical techniques have claimed a variety of ground states. On the one hand, density-matrix renormalization group (DMRG) calculations have claimed for a fully gapped (non-chiral) $\mathbb{Z}_2$ topological spin-liquid ground state that does not break any point group symmetry. [13, 14] On the other hand, an algebraic and fully symmetric $U(1)$ Dirac spin liquid has been proposed as the ground state, by using projected fermionic wave functions and variational Monte Carlo (VMC) approach. [15–20] In addition, valence bond crystals have been suggested from many other techniques. In particular, a 36-site unit cell valence-bond crystal [21–23] was proposed using quantum dimer models, [24–28] series expansion [29, 30] and multi-scale entanglement renormalization Ansatz (MERA) [31] techniques. Finally, a recent coupled cluster method (CCM) suggested a $q = 0$ (uniform) state. [32]

On general theoretical grounds, the $\mathbb{Z}_2$ spin liquids in two spatial dimensions are known to be stable phases, [47–49] as compared to algebraic $U(1)$ spin liquids, which are known to be only marginally stable. [50] However, explicit numerical calculations using projected wave functions have shown the $U(1)$ Dirac spin liquid to be stable (locally and globally) with respect to dimerizing into all known valence-bond crystal phases. [15, 17, 18, 20] Furthermore, it was shown that, within this class of Gutzwiller projected wave functions, all the fully symmetric, gapped $\mathbb{Z}_2$ spin liquids have a higher energy compared to the $U(1)$ Dirac spin liquid. [19, 51]

On the experimental front, the kagome spin-1/2 QHAF model is well reproduced in Herbertsmithite ($ZnCu_3(OH)_6Cl_2$), a compound with perfect kagome lattice geometry. [33–42] All experimental probes on Herbertsmithite point towards a spin-liquid behavior down to 20mK (i.e., four orders of magnitude smaller than the super-exchange coupling), which was established on the magnesium version of Herbertsmithite ($MgCu_3(OH)_6Cl_2$). [43–45] Raman spectroscopic studies give further hints towards a gapless (algebraic) spin liquid. [46]

In this letter, we systematically improve the projected fermionic wave functions of the $U(1)$ Dirac and other competing spin liquids by applying a few Lanczos steps on large clusters, implemented stochastically within a variational Monte Carlo method. [52] We perform a zero-variance extrapolation of the energy and the static spin structure factor, which enables us to extract their exact values in the ground state on large cluster sizes and obtain an accurate estimate of the thermodynamic limit. In addition, we use Green's function Monte Carlo method, with the fixed-node (FN) approximation, [53] to extract the physical properties of the true ground state. Our main result is to show that the $U(1)$ gapless spin liquid has an energy quite close to recent DMRG estimates, [13, 14] thus representing a very competitive state for the spin-1/2 QHAF on the kagome lattice (if not the true ground state).

Model, wave functions, and numerical techniques.

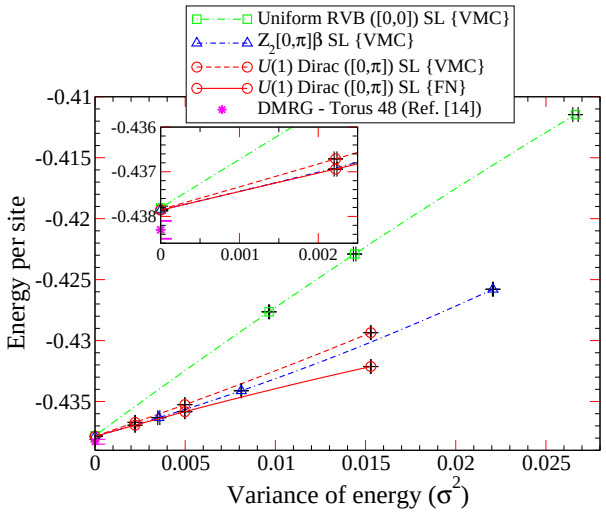

FIG. 1. (Color online) Variational energies of the 48-site cluster as a function of the variance of the energy, for zero, one and two Lanczos steps. The ground-state energy is estimated by extrapolating the three variational results to the zero-variance limit by a quadratic fit. Three different starting wave functions are used. The $U(1)$ Dirac spin liquid has also been studied using FN approximation.

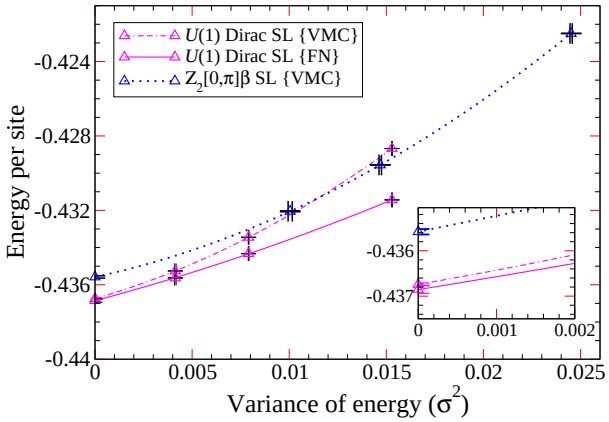

FIG. 2. (Color online) The same as in Fig. 1 for the 192-site cluster. Here, only $\mathbb{Z}_2[0,\pi]\beta$ and $U(1)$ Dirac states have been considered.

The Hamiltonian for the spin-1/2 quantum Heisenberg antiferromagnetic model is:

$$\hat{\mathcal{H}} = J \sum_{\langle ij \rangle} \hat{\mathbf{S}}_i \cdot \hat{\mathbf{S}}_j \qquad (1)$$

where $J > 0$ and $\langle ij \rangle$ denotes sum over nearest-neighbor pairs of sites. The $\hat{\mathbf{S}}_i$ are spin-1/2 operators at each site i. All energies will be given in units of J.

The physical variational wave functions are defined by

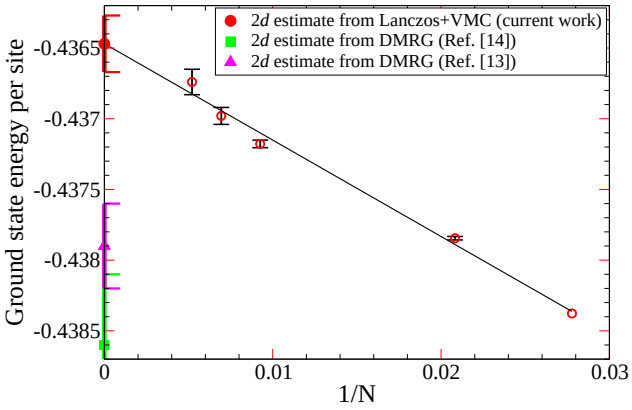

FIG. 3. (Color online) The thermodynamic estimate of the ground-state energy obtained by a finite size extrapolation of the estimated ground-state energies (see Table I). The energy on the 36-site cluster is from exact diagonalization. Comparison is also made with recent DMRG estimates. [13, 14]

projecting non-correlated fermionic states:

$$|\Psi_{\rm VMC}(\chi_{ij},\Delta_{ij},\mu,\zeta)\rangle = \mathcal{P}_{\mathbf{G}}|\Psi_{\rm MF}(\chi_{ij},\Delta_{ij},\mu,\zeta)\rangle, \qquad (2)$$

where $\mathcal{P}_{\mathbf{G}} = \prod_i (1 - n_{i,\uparrow} n_{i,\downarrow})$ is the full Gutzwiller projector enforcing the one fermion per site constraint. Here, $|\Psi_{\rm MF}(\chi_{ij},\Delta_{ij},\mu,\zeta)\rangle$ is the ground state of a mean-field Hamiltonian constructed out of Abrikosov fermions and containing hopping, chemical potential, and singlet pairing terms:

$$\hat{\mathcal{H}}_{\rm MF} = \sum_{i,j,\alpha} (\chi_{ij} + \mu\delta_{ij}) \hat{c}^{\dagger}_{i,\alpha} \hat{c}_{j,\alpha} + \sum_{i,j} \{ (\Delta_{ij} + \zeta\delta_{ij}) \hat{c}^{\dagger}_{i,\uparrow} \hat{c}^{\dagger}_{j,\downarrow} + h.c. \}, \qquad (3)$$

where $\alpha = \uparrow, \downarrow$, $\chi_{ij} = \chi^{*}_{ji}$ and $\Delta_{ij} = \Delta_{ji}$. Besides the chemical potential μ, we also consider real and imaginary components of on-site pairing, which are absorbed in ζ. The spin-liquid phases are characterized by different patterns of distribution of the underlying gauge fluxes through the plaquettes which are implemented by a certain distribution of the phases of χ_{ij} and Δ_{ij} on the lattice links, in addition one also needs to specify the on-site terms μ and ζ. [48, 54]

Here, we want to improve previous variational calculations and approach, in a systematic way, the true ground state. This task can be achieved by the application of Lanczos steps: [52]

$$|\Psi_{p-\rm LS}\rangle = \left(1 + \sum_{k=1}^{p} \alpha_k \hat{\mathcal{H}}^k\right) |\Psi_{\rm VMC}\rangle \qquad (4)$$

where the α_k's are additional variational parameters. The convergence of $|\Psi_{p-\rm LS}\rangle$ to the exact ground state

$|\Psi_{\rm ex}\rangle$ is guaranteed for large p provided the starting state is not orthogonal to $|\Psi_{\rm ex}\rangle$, i.e., for $\langle\Psi_{\rm ex}|\Psi_{\rm VMC}\rangle \neq 0$. However, on large cluster sizes, only a few steps can be efficiently performed and here we consider the case with $p = 1$ and $p = 2$ ($p = 0$ corresponds to the original starting variational wave function). Subsequently, an estimate of the exact ground-state energy may be achieved by the method of variance extrapolation: for sufficiently accurate states, we have that $E \approx E_{\rm ex} + \text{constant} \times \sigma^2$, where $E = \langle\hat{\mathcal{H}}\rangle/N$ and $\sigma^2 = (\langle\hat{\mathcal{H}}^2\rangle - \langle\hat{\mathcal{H}}\rangle^2)/N$ are the energy and variance per site, respectively. Whence, the exact ground-state energy $E_{\rm ex}$ can be extracted by fitting E vs σ^2 for $p = 0$, 1, and 2.

The energy, its variance, and other physical properties of the wave functions corresponding to $p = 0$, 1, and 2 Lanczos steps are obtained using standard VMC method. Moreover, the pure variational approach may be improved by using the FN approach, in which the high-energy components of the variational wave function are (partially) filtered out. [53] In particular, in the FN Monte Carlo method, the ground state of an auxiliary FN Hamiltonian is obtained and the approximation consists in assigning the nodal surface *a priori*, based upon a given guiding wave function, which is generally the best variational state. The energies obtained in this way are variational, [53] and hence we have a controlled approximation of the original problem. Here, the guiding wave function is obtained by optimizing the mean-field state of Eq. (2) using the method described in Refs. [55, 56]. Then, we find the best Lanczos parameters α_p and finally we perform the VMC and FN Monte Carlo calculations for $|\Psi_{p-\rm LS}\rangle$ with $p = 0$, 1, and 2.

Results. We performed our variational calculations on toric clusters with mixed periodic-antiperiodic boundary conditions on the mean-field Hamiltonian of Eq. (3), which ensure non-degenerate wave functions at half filling. We first consider the 48-site cluster (i.e., $4 \times 4 \times 3$). As our starting ($p = 0$) variational wave functions, we take three different spin liquids, namely, (i) the $U(1)$ Dirac spin liquid, which has a Fermi surface consisting of two points. [15, 16] The structure of the wave function is such that 10% of the configurations $|x\rangle$ (in which electrons reside on different sites of the lattice with given spin along the z direction) have zero weight (i.e., $\langle x|\Psi\rangle = 0$). (ii) The uniform RVB spin liquid, which consists of a large circular spinon Fermi surface, [17] and has 35% of the configurations with zero weight. (iii) The $\mathbb{Z}_2[0,\pi]\beta$ spin liquid, which is fully gapped [57] and has a negligible (0.001%) number of configurations with zero weight. The zero-weight configurations are not visited by the random walk in the variational Monte Carlo method. The effect of two Lanczos steps on these wave functions is shown in Fig. 1 (see also Table I for the actual values of the energies of the $U(1)$ Dirac state). Our estimate of the ground-state energy on the 48-site cluster is thus $E/J = -0.437845(4)$, which is comparable with the DMRG estimate on a torus. [14, 58] Also the best *pure* variational energies are comparable within the two methods, see Table I. We want to stress the fact that the extrapolated energy is the same (within error bars) upon starting from all three wave functions. This is mainly due to the fact that, on relatively small clusters, few Lanczos steps are enough to filter out the high-energy components of the initial wave function and get a good estimation of the ground-state energy.

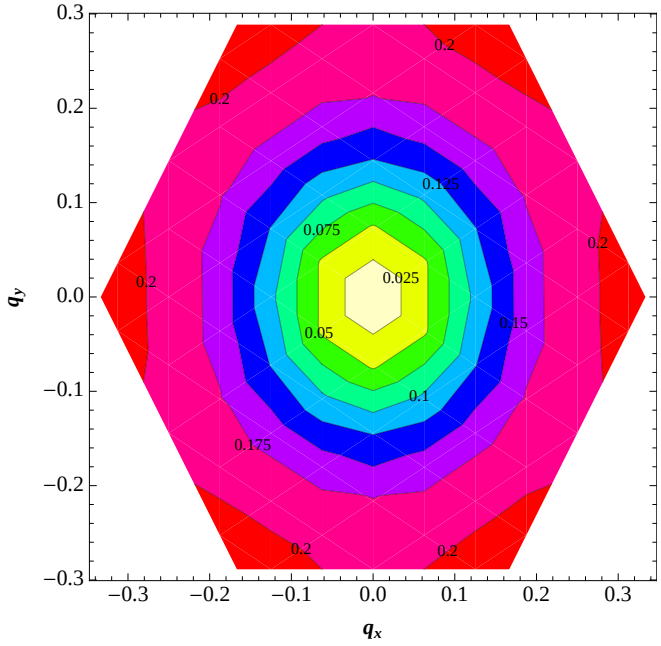

FIG. 4. (Color online) Intensity plot of the static spin structure factor $S(\mathbf{q})$ on the 192-site cluster.

On larger sizes, the extrapolations of $U(1)$ and $\mathbb{Z}_2[0,\pi]\beta$ states deviate, the former one giving a slightly lower extrapolation, see Fig. 2 for the 192-site cluster. This fact suggests that the actual ground state is better described by a gapless algebraic $U(1)$ Dirac state, rather than a gapped topological $\mathbb{Z}_2$ spin liquid, as reported by DMRG calculations. In the following, for obtaining the ground-state energies on larger clusters we used only the $U(1)$ Dirac wave function as the starting variational state. In Table I, we report our best results on different clusters (see the Supplementary Material for plots of the variance extrapolations on 108- (see Fig. 6) and 144-site (see Fig. 7) clusters. Also see Fig. 8). We would like to emphasize that our best variational energy on a 108-site cluster is significantly lower compared to the corresponding DMRG one, see Table I.

By using the ground-state energy estimates on different cluster sizes, we performed a finite size extrapolation, see Fig. 3. Our final estimate for the energy of the infinite two-dimensional system is:

$$E_\infty^{2D}/J = -0.4365(2). \tag{5}$$

Size	0-LS	1-LS	2-LS	0-LS + FN	1-LS + FN	2-LS + FN	Var. DMRG	Est. Ground State
48	−0.4293510(4)	−0.4352562(3)	−0.436712(1)	−0.432130(2)	−0.435834(3)	−0.436942(2)	−0.4366	**−0.437845(4)**
108	−0.4287665(4)	−0.4341032(5)	−0.435787(3)	−0.431507(1)	−0.434823(2)	−0.436072(1)	−0.4316	**−0.437178(9)**
144	−0.4286959(5)	−0.4337616(4)	−0.435515(4)	−0.4314455(8)	−0.434544(2)	−0.435839(9)		**−0.43698(2)**
192	−0.4286749(4)	−0.4334481(5)	−0.435255(4)	−0.431437(2)	−0.434325(4)	−0.435633(8)		**−0.43674(3)**

TABLE I. Energies of the $U(1)$ Dirac spin liquid with $p = 0$, 1, and 2 Lanczos steps on different cluster sizes obtained by variational and FN Monte Carlo are given. In the penultimate column, we report the best *variational* DMRG energies. [59] The ground-state energy of the spin-1/2 QHAF estimated by us using zero-variance extrapolation of VMC energy values on different cluster sizes is marked in bold.

This estimate is slightly higher (see Fig. 3) compared to DMRG extrapolations of Refs. [13, 14]. However, an energy estimate which is slightly lower by only few error-bars does not necessarily mean it is more accurate. We would like to stress that the same value for the extrapolated energy is obtained by using the FN approach (see Fig. 9 in the Supplementary Material). Moreover, it is worth mentioning that our energies are obtained with a state that has all the symmetries of the lattice, while DMRG states are non-uniform (due to boundary effects).

Let us now move to the calculation of the spin-spin correlations, which is defined by:

$$\mathrm{S}(\mathbf{q}) = \frac{1}{\mathrm{N}} \sum_{ij} \sum_{\mathbf{R}} e^{-\imath \mathbf{q}\cdot\mathbf{R}} \mathrm{S}_{ij}(\mathbf{R}), \qquad (6)$$

where N is the total number of sites, $i, j = 1$, 2, and 3 label the three sites in the unit cell, $\mathbf{R}$ defines the Bravais lattice, and $\mathrm{S}_{ij}(\mathbf{R})$ is the real space spin-spin correlation function.

The $U(1)$ Dirac spin liquid is characterized by a power law ($\sim 1/r^4$) decay of real space, long distance spin-spin correlations. [16] Here, we study the evolution of its static spin structure factor $\mathrm{S}(\mathbf{q})$ on the 192-site cluster under the action of one and two Lanczos steps and zero-variance extrapolation. Our estimate of the ground-state $\mathrm{S}(\mathbf{q})$ is obtained by a zero-variance extrapolation, see Fig. 11 in the Supplementary Material. The corresponding intensity plot of the extrapolated $\mathrm{S}(\mathbf{q})$ is shown in Fig. 4. One can clearly see that at large $\mathbf{q}$, the spectral weight is concentrated on the corners of the hexagon, not very differently from what is found in a recent DMRG study. [14] However, what really matters is the behavior of $\mathrm{S}(\mathbf{q})$ for small $\mathbf{q}$ (namely at long distance). Although the application of few Lanczos steps may not be sufficient to change the long-distance properties (because the Hamiltonian is a local operator), our calculations show that $\mathrm{S}(\mathbf{q})$ at small $\mathbf{q}$ remains practically unchanged under the action of one or two Lanczos steps and the subsequent zero-variance extrapolation (see Figs. 10 and 12 in the Supplementary Material).

Summary. In summary, our systematic numerical study shows that competitive variational wave functions based upon Abrikosov fermions may be obtained. Indeed, our estimation for the energy of a gapless (algebraic) $U(1)$ Dirac spin liquid is very close to the recent DMRG results, [13, 14] which supported a fully gapped $\mathbb{Z}_2$ topological spin-liquid ground state. In this respect, our results lend support to the view that the exotic algebraic spin liquid can in fact occur as a true ground state of the spin-1/2 QHAF on the kagome lattice. Very recently, other approximate approaches proposed alternative ground states with broken symmetries. [60, 61]

We would like to mention that a further improvement of the variational wave function would require an introduction of local monopole fluctuations over the static mean-field state of Eq. (3). On small system sizes, such fluctuations were shown to lower the energy of the system within the Schwinger boson approach. [62] However, on large clusters, it is extremely difficult to construct workable wave functions with (even static) topological defects. It is worth mentioning that the possibility of another energetically competing state entering the game remains open, this is a chiral $\mathbb{Z}_2$ topological spin liquid [63] which has been proposed as the ground state within a Schwinger boson mean-field theory, [64] but whose projected wave function study remains to be done on large clusters such as 48 sites so as to enable a comparison with the $U(1)$ Dirac spin liquid. Finally, the projected wave functions can also be constructed for chiral valence-bond crystal phases and it would be interesting to study their energetics, especially in light of the fact that they have been proposed as a competing ground state using generalized quantum dimer models. [28]

Acknowledgements YI and DP acknowledge support from the 'Agence Nationale de la Recherche' under grant no. ANR 2010 BLANC 0406-0. We are grateful for the permission granted to access the HPC resources of CALMIP under the allocation 2012-P1231.

* yiqbal@ictp.it
† becca@sissa.it
‡ sorella@sissa.it
§ didier.poilblanc@irsamc.ups-tlse.fr

[1] P. W. Anderson, Mater. Res. Bull. **8**, 153 (1973).
[2] P. W. Anderson, Science. **235**, 1196 (1987).
[3] L. Balents, Nature. **464**, 199 (2010).
[4] V. Elser, Phys. Rev. Lett. **62**, 2405 (1989).

[5] P. Lecheminant, B. Bernu, C. Lhuillier, L. Pierre, and P. Sindzingre, Phys. Rev. B **56**, 2521 (1997).
[6] P. Sindzingre and C. Lhuillier, EPL **88**, 27009 (2009).
[7] H. Nakano and T. Sakai, J. Phys. Soc. Jpn. **80**, 053704 (2011).
[8] A. M. Läuchli, J. Sudan, and E. S. Sørensen, Phys. Rev. B **83**, 212401 (2011).
[9] R. R. P. Singh and D. A. Huse, Phys. Rev. Lett. **68**, 1766 (1992).
[10] G. Misguich and B. Bernu, Phys. Rev. B **71**, 014417 (2005).
[11] L. Dang, S. Inglis, and R. G. Melko, Phys. Rev. B **84**, 132409 (2011).
[12] L. Balents, M. P. A. Fisher, and S. M. Girvin, Phys. Rev. B **65**, 224412 (2002).
[13] S. Yan, D. A. Huse, and S. R. White, Science. **332**, 1173 (2011).
[14] S. Depenbrock, I. P. McCulloch, and U. Schollwöck, Phys. Rev. Lett. **109**, 067201 (2012).
[15] Y. Ran, M. Hermele, P. A. Lee, and X. G. Wen, Phys. Rev. Lett. **98**, 117205 (2007).
[16] M. Hermele, Y. Ran, P. A. Lee, and X. G. Wen, Phys. Rev. B **77**, 224413 (2008).
[17] O. Ma and J. B. Marston, Phys. Rev. Lett. **101**, 027204 (2008).
[18] Y. Iqbal, F. Becca, and D. Poilblanc, Phys. Rev. B **83**, 100404(R) (2011).
[19] Y. Iqbal, F. Becca, and D. Poilblanc, Phys. Rev. B **84**, 020407(R) (2011).
[20] Y. Iqbal, F. Becca, and D. Poilblanc, New. J. Phys. (in press), arXiv: 1203.3421 (2012) [cond.mat].
[21] J. B. Marston and C. Zeng, J. Appl. Phys. **69**, 5962 (1991).
[22] P. Nikolic and T. Senthil, Phys. Rev. B **68**, 214415 (2003).
[23] K. Hwang, Y. B. Kim, J. Yu, and K. Park, Phys. Rev. B **84**, 205133 (2011).
[24] C. Zeng and V. Elser, Phys. Rev. B **51**, 8318 (1995).
[25] D. Poilblanc, M. Mambrini, and D. Schwandt, Phys. Rev. B **81**, 180402(R) (2010).
[26] D. Schwandt, M. Mambrini, and D. Poilblanc, Phys. Rev. B **81**, 214413 (2010).
[27] A. Ralko and D. Poilblanc, Phys. Rev. B **82**, 174424 (2010).
[28] D. Poilblanc and G. Misguich, Phys. Rev. B **84**, 214401 (2011).
[29] R. R. P. Singh and D. A. Huse, Phys. Rev. B **76**, 180407(R) (2007).
[30] R. R. P. Singh and D. A. Huse, Phys. Rev. B **77**, 144415 (2008).
[31] G. Evenbly and G. Vidal, Phys. Rev. Lett. **104**, 187203 (2010).
[32] O. Götze, D. J. J. Farnell, R. F. Bishop, P. H. Y. Li, and J. Richter, Phys. Rev. B **84**, 224428 (2011).
[33] M. P. Shores, E. A. Nytko, B. M. Bartlett, and D. G. Nocera, J. Am. Chem. Soc. **127**, 13462 (2005).
[34] O. Ofer, A. Keren, E. A. Nytko, M. P. Shores, B. M. Bartlett, D. G. Nocera, C. Baines, and A. Amato, arXiv: 0610540 (2006) [cond.mat].
[35] F. Bert, S. Nakamae, F. Ladieu, D. L'Hôte, P. Bonville, F. Duc, J. C. Trombe, and P. Mendels, Phys. Rev. B. **76**, 132411 (2007).
[36] S. H. Lee, H. Kikuchi, Y. Qiu, B. Lake, Q. Huang, K. Habicht, and K. Kiefer, Nature Mater. **6**, 853 (2007).
[37] P. A. Lee, Science Perspectives. **321**, 1306 (2008).
[38] M. A. de Vries, K. V. Kamenev, W. A. Kockelmann, J. Sanchez-Benitez, and A. Harrison, Phys. Rev. Lett. **100**, 157205 (2008).
[39] T. Imai, E. A. Nytko, B. M. Bartlett, M. P. Shores, and D. G. Nocera, Phys. Rev. Lett. **100**, 077203 (2008).
[40] A. Olariu, P. Mendels, F. Bert, F. Duc, J. C. Trombe, M. A. de Vries, and A. Harrison, Phys. Rev. Lett. **100**, 087202 (2008).
[41] P. Mendels and F. Bert, J. Phys. Soc. Jpn. **79**, 011001 (2010).
[42] T. H. Han, J. S. Helton, S. Chu, A. Prodi, D. K. Singh, C. Mazzoli, P. Müller, D. G. Nocera, and Y. S. Lee, Phys. Rev. B **83**, 100402(R) (2011).
[43] P. Mendels, F. Bert, M. A. de Vries, A. Olariu, A. Harrison, F. Duc, J. C. Trombe, J. S. Lord, A. Amato, and C. Baines, Phys. Rev. Lett. **98**, 077204 (2007).
[44] J. S. Helton, K. Matan, M. P. Shores, E. A. Nytko, B. M. Bartlett, Y. Yoshida, Y. Takano, A. Suslov, Y. Qiu, J. H. Chung, D. G. Nocera, and Y. S. Lee, Phys. Rev. Lett. **98**, 107204 (2007).
[45] E. Kermarrec, P. Mendels, F. Bert, R. H. Colman, A. S. Wills, P. Strobel, P. Bonville, A. Hillier, and A. Amato, Phys. Rev. B **84**, 100401 (2011).
[46] D. Wulferding, P. Lemmens, P. Scheib, J. Röder, P. Mendels, S. Chu, T. Han, and Y. S. Lee, Phys. Rev. B **82**, 144412 (2010).
[47] S. Sachdev, Phys. Rev. B **45**, 12377 (1992).
[48] X. G. Wen, Phys. Rev. B **65**, 165113 (2002).
[49] G. Misguich, D. Serban, and V. Pasquier, Phys. Rev. Lett. **89**, 137202 (2002).
[50] M. Hermele, T. Senthil, M. P. A. Fisher, P. A. Lee, N. Nagaosa, and X. G. Wen, Phys. Rev. B **70**, 214437 (2004).
[51] F. Yang and H. Yao, Phys. Rev. Lett. **109**, 147209 (2012).
[52] S. Sorella, Phys. Rev. B **64**, 024512 (2001).
[53] D. F. B. ten Haaf, H. J. M. van Bemmel, J. M. J. van Leeuwen, W. van Saarloos, and D. M. Ceperley, Phys. Rev. B **51**, 13039 (1995).
[54] X. G. Wen, Phys. Rev. B **44**, 2664 (1991).
[55] S. Sorella, Phys. Rev. B **71**, 241103 (2005).
[56] S. Yunoki and S. Sorella, Phys. Rev. B **74**, 014408 (2006).
[57] Y. M. Lu, Y. Ran, and P. A. Lee, Phys. Rev. B **83**, 224413 (2011).
[58] H. C. Jiang, Z. Y. Weng, and D. N. Sheng, Phys. Rev. Lett. **101**, 117203 (2008).
[59] On the 48-site torus, $E/J = -0.4366$ corresponds to $m = 3000$ states in the $SU(2)$ implementation of DMRG (U. Schollwöck, Private Communication). Recent unpublished calculations by S. R. White using the $U(1)$ implementation of DMRG give an energy per site of $E/J = -0.4381$ for $m = 19860$ states (Private Communication). On the 108-site torus, $E/J = -0.4316$ corresponds to $m = 6000$ states in the $U(1)$ DMRG of Ref. 58. The $SU(2)$ DMRG with $m = 1400$ states gives $E/J = -0.4285$ (U. Schollwöck, Private Communication). The best extrapolated ground state energy estimate from DMRG on the 48-site torus is $E/J = -0.4383(2)$ and on the 108-site torus is $E/J = -0.4383(3)$, see Ref. 14.
[60] B. K. Clark, J. M. Kinder, E. Neuscamman, G. K.-L. Chan, and M. J. Lawler, arXiv: 1210.1585 (2012) [cond.mat].
[61] S. Capponi, V. Ravi Chandra, A. Auerbach, and M. Weinstein, arXiv: 1210.5519 (2012) [cond.mat].
[62] T. Tay and O. I. Motrunich, Phys. Rev. B **84**, 193102

(2011).
[63] K. Yang, L. K. Warman, and S. M. Girvin, Phys. Rev. Lett. **70**, 2641 (1993).
[64] L. Messio, B. Bernu, and C. Lhuillier, Phys. Rev. Lett. **108**, 207204 (2012).

Supplementary Material

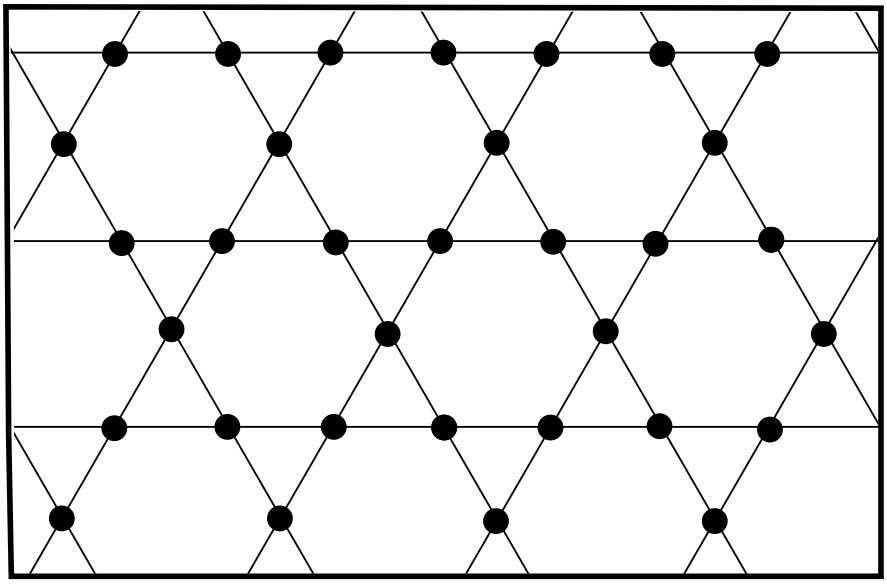

FIG. 5. A lattice of corner sharing triangles giving rise to two elementary plaquettes, the triangle and the hexagon. The kagome lattice is the most frustrated among the 11 Archimedean tilings possible in $2D$ and has a coordination number of 4.

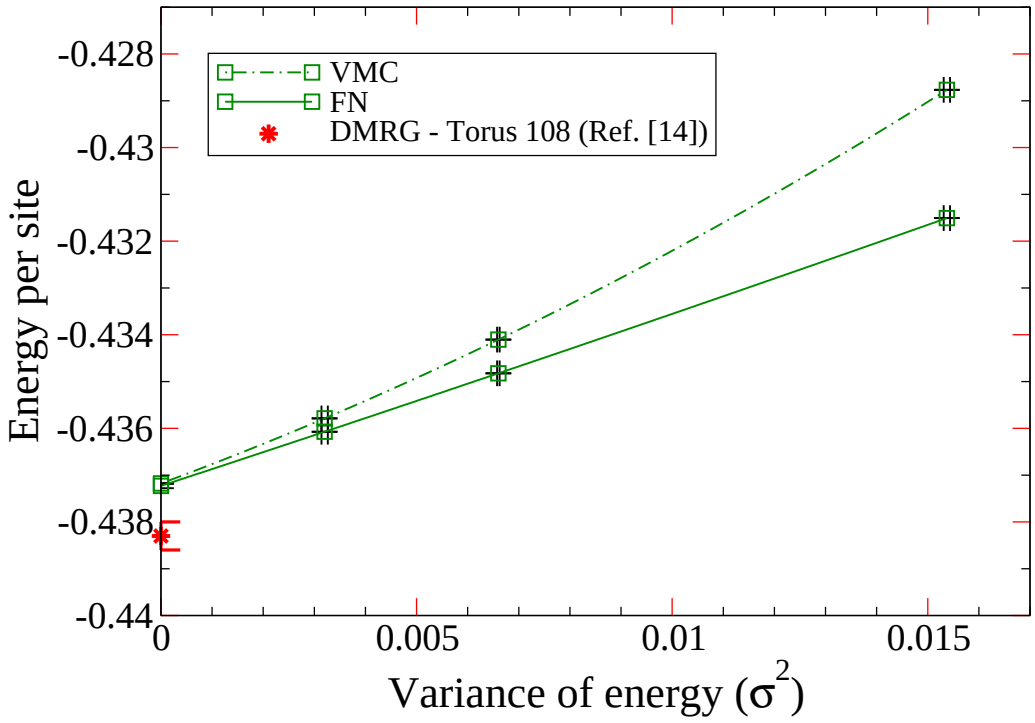

FIG. 6. (Color online) The same as in Fig. 1 of the main paper, for the 108-site cluster. Here, only the $U(1)$ Dirac state is considered and has been studied using both variational and fixed-node Monte Carlo methods.

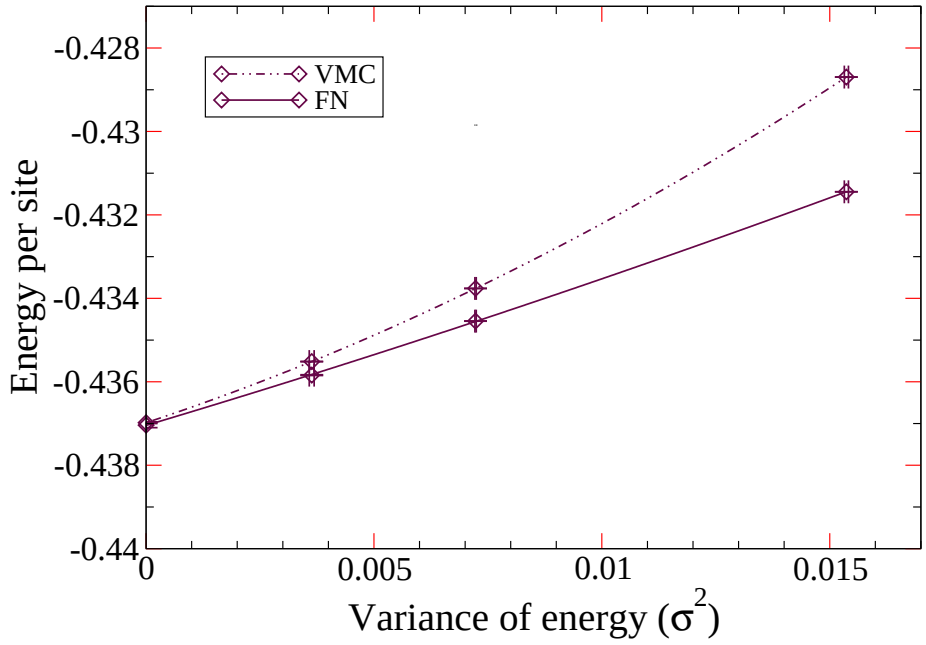

FIG. 7. (Color online) The same as in Fig. 1 of the main paper, for the 144-site cluster. Here, only the $U(1)$ Dirac state is considered and has been studied using both variational and fixed-node Monte Carlo methods.

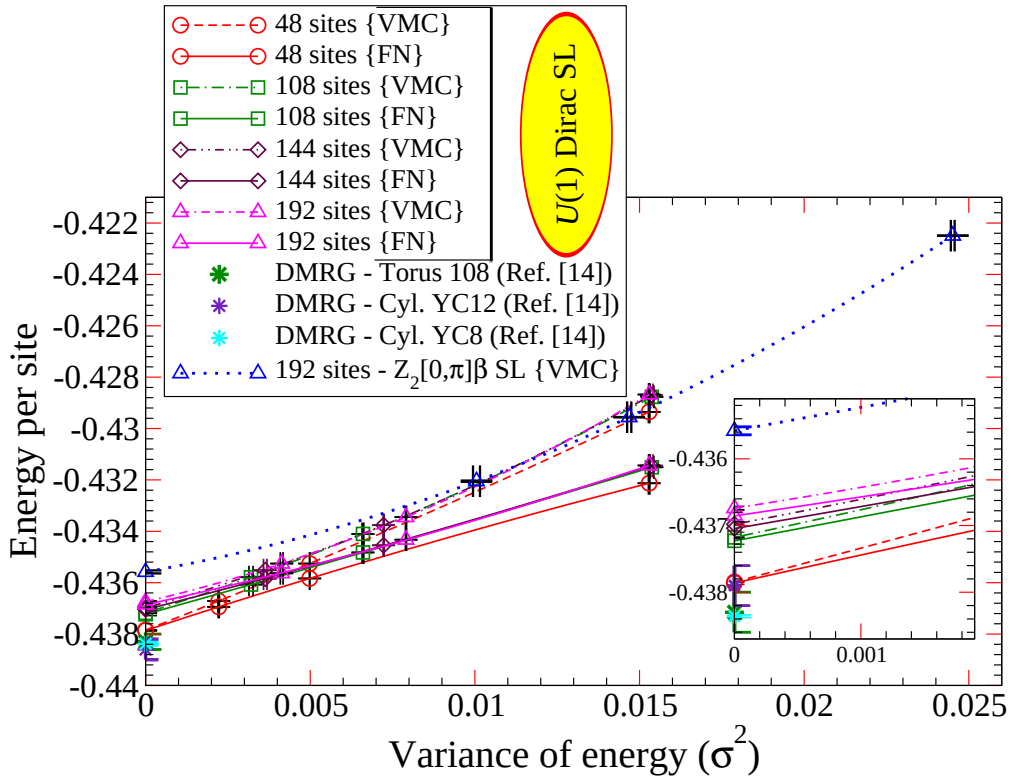

FIG. 8. (Color online) The variance extrapolations on all cluster sizes for different starting variational wave functions are shown together for comparison. The inset shows the magnification near zero-variance. Note: The magnitude of the pairing in the $\mathbb{Z}_2[0,\pi]\beta$ SL Ansätz is fixed to unity.

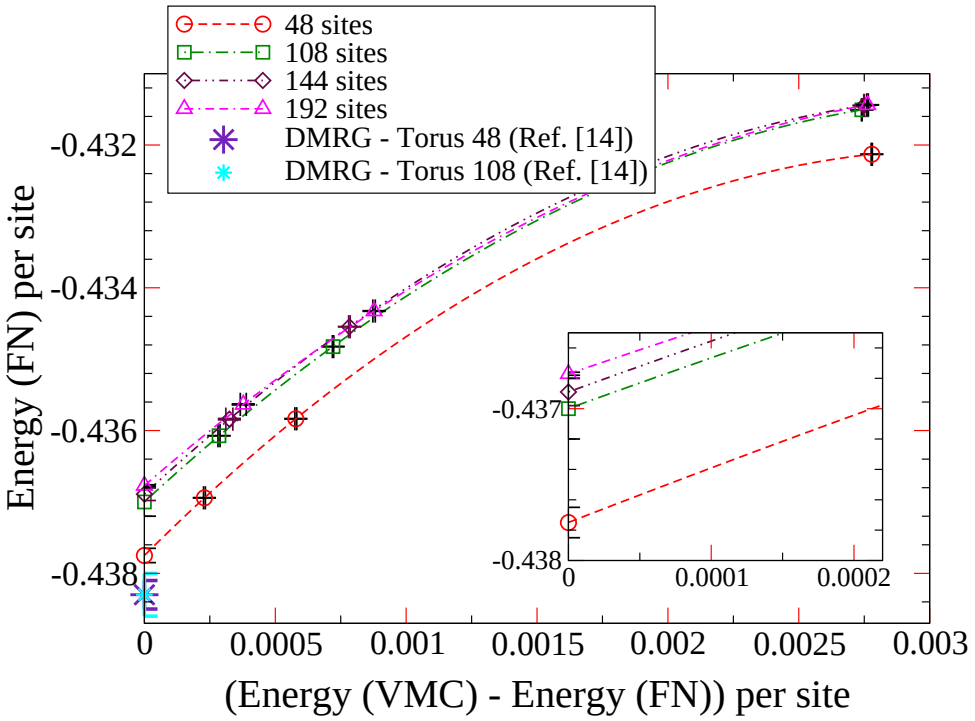

FIG. 9. (Color online) For all four cluster sizes, the fixed-node Monte Carlo energies have been extrapolated to the zero of the difference $E_{\mathrm{VMC}} - E_{\mathrm{FN}}$. The extrapolated values are within error bars of the zero-variance extrapolated values given in Table. I of the main paper, this shows that the VMC estimates are exact.

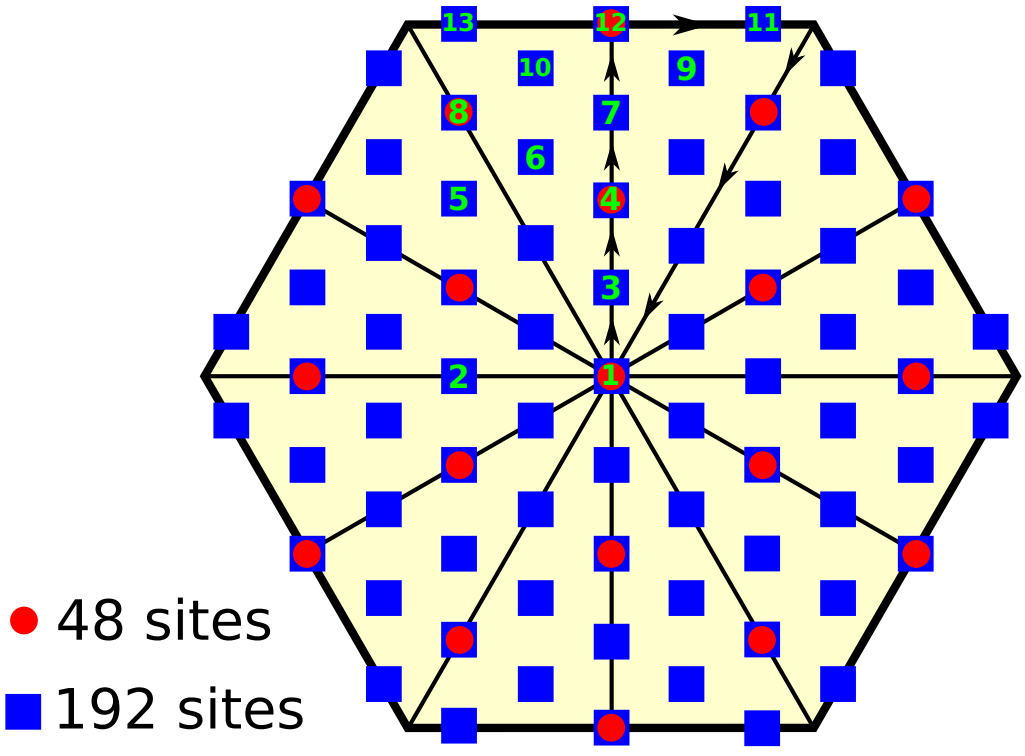

FIG. 10. (Color online) The Brillouin zone and the available crystal momenta for the 48 and the 192 site clusters are marked. Also, the 13 inequivalent momenta for the 192 site cluster are labelled with numbers.

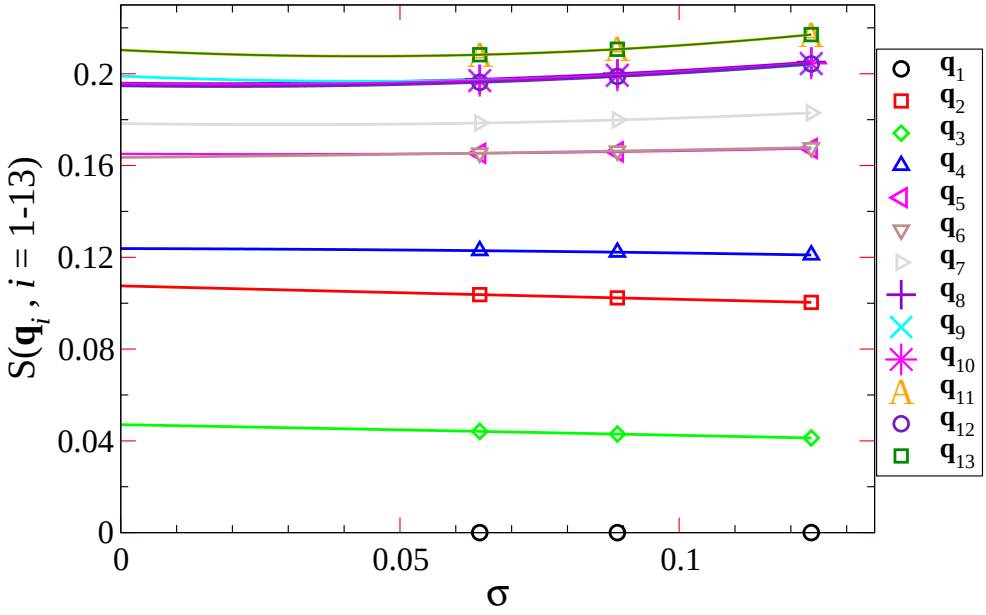

FIG. 11. (Color online) Quadratic fit of zero-σ extrapolation of the S($\mathbf{q}$) for the 13 inequivalent momenta on the 192-site cluster. The starting wave function is the $U(1)$ Dirac spin liquid on which one and two Lanczos steps have been performed. The numbering of the momenta is according to the above given Fig. 6.

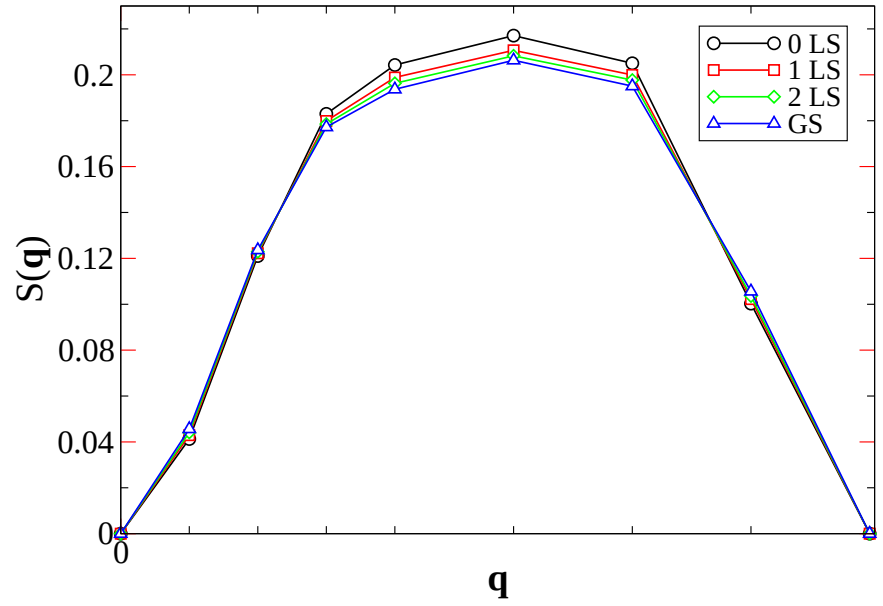

FIG. 12. (Color online) On the 192-site cluster, the S($\mathbf{q}$) are plotted for the $\mathbf{q}$ points lying on the path marked with arrows in the Brillouin zone, namely for the $U(1)$ Dirac spin liquid and the corresponding wave functions obtained by applying one, and two Lanczos steps on it, and also the extrapolated ground state. The error bars of S($\mathbf{q}$) are of the order of 10^{-4}.